

[Original article]

Liquid phase adsorption of dyes and dextrans by crystallized mesoporous wood carbon obtained by nickel-catalyzed carbonization of larch at 900°C

Tsutomu Suzuki* *****, Kyoko Suzuki*, Kazuyuki Hattori*, Noriyasu Okazaki*,
Yukie Saito**, Hidetoshi Kita***, Hisashi Tamai****

Abstract: For crystallized mesoporous carbon (CMC) obtained by carbonization of nickel-loaded larch at 900°C, its liquid phase adsorption capacity for dyes and dextrans was examined before and after pulverization followed by washing with acid. By pulverization, graphitic nano shell chains as the crystallized form of CMC were fragmented into raspberry-shaped nano shell carbon particles accompanying the increase of mesopore volume and width. These morphological and pore structural changes brought about great increase in the adsorption amounts of both adsorbates. Subsequent washing with acid to remove coexisting nickel led to further increase in the amount of dextrans to surpass commercial mesoporous carbon in the adsorption capacity, although it was disadvantageous for the adsorption of dyes. As removal of the metal for its recovery and reuse is also industrially preferable, pulverization and subsequent washing with acid were post-treatments suitable for practical production of an adsorbent for non-polar polymers from CMC.

Keywords: crystallized mesoporous wood carbon, graphitic nano shell chain, liquid phase adsorption, pulverization, washing with acid

1. Introduction

Nickel-catalyzed carbonization of wood at 900°C has been developed in our laboratory for coproduction of functional carbon and fluid fuels¹⁻⁵⁾. This process deserves special attention for easy and efficient production of crystallized mesoporous carbon^{1,2,6)} (abbreviated as CMC) that has two potential functions of electroconductivity and liquid phase adsorption for macromolecules. It should be emphasized in this connection that such a dual function has never been reported for carbonaceous materials, including wood carbon, until then to our knowledge. This will predict a quite unique microstructure of CMC. Actually SEM and TEM observations of CMC subjected to washing with acid followed by atmospheric oxidation at below 500°C for removal of nickel and amorphous

carbon, respectively, revealed⁷⁾: the crystal region was an aggregate of graphitic nano shell (equivalent to 'hollow') chains (GNSC) looking like a tangle of worms and each chain was a long winding string of nano shell carbons (NSC) with the surface of several graphite layers, as displayed in Fig. 1. Furthermore, the SEM image disclosed that a number of the space

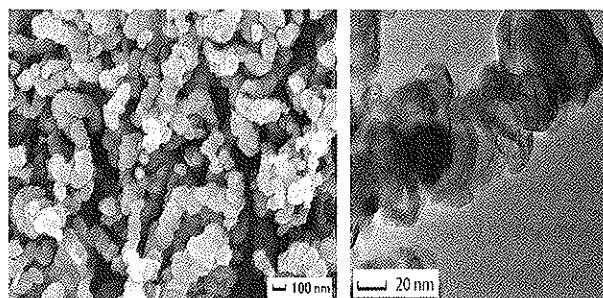


Fig. 1 Typical SEM (left) and TEM (right) images of graphitic nano shell chains (GNSC) derived from crystallized mesoporous carbon prepared by nickel-catalyzed carbonization of larch at 900°C.

* Departments of Biotechnology and Environmental Chemistry, Kitami Institute of Technology, Japan

** Graduate School of Agricultural and Life Science, The University of Tokyo, Japan

*** Graduate School of Science and Engineering, Yamaguchi University, Japan

**** Graduate School of Engineering, Hiroshima University, Japan

*****Corresponding author: 165 Koen-cho, Kitami, Hokkaido 090-8507, Japan, e-mail: suzuki@serv.chem.kitami-it.ac.jp

and voids among individual GNSC were equal to mesopore (2-50 nm in diameter) in size. It followed that a large proportion of mesopore was generated during the formation of GNSC to leave it in the crystal region, thereby explaining how and why the dual function can develop⁷⁾. It was also found that the shell chains appeared only in the cell wall tissue to be covered with amorphous carbon, as illustrated later in Fig. 5.

In parallel with such clarification of the unique microstructure, trials to develop practical carbon products by introducing post-treatments are now in progress. For example, in the application as conductive filler, raw CMC was pulverized and washed with acid prior to blending with non-conductive matrix like plastics^{8,9)}. The filler ability enhanced after these treatments primarily due to increase in the crystallinity of carbon, so that it was comparable to that of a commercial conductive carbon, a sort of acetylene black called Denka black^{7,10)}. When the above atmospheric oxidation was subsequently applied, the remaining carbon exclusively occupied by GNSC surpassed the commercial acetylene black in the ability⁷⁾. These results ensured a good substitute of CMC for the current petroleum-derived conductive carbon. On the contrary, influence of these pretreatments, which are to be likewise incorporated for producing a liquid phase adsorbent for macromolecules, on the adsorption capacity is not systematically examined yet. The present study thus deals with this subject by paying chief attention to morphological and pore structural changes of CMC. The capacity was evaluated and discussed by comparing with those of commercial activated carbons.

2. Experimental

2.1 Material

Nickel-loaded wood carbon (NiWC) equivalent to CMC was prepared by previously described carbonization of powdered larch (0.6-1.4 mm in

diameter) loaded with 2 wt% nickel in a flow of nitrogen at 900°C for 1h²⁾. None-loaded wood carbon (NoWC) as control was obtained by applying the same carbonization conditions. For comparison, two commercial activated carbons were chosen: one was 'Granular Shirasagi G2X' used for gas adsorption and another was 'Charcoal, activated for chromatography (Wako Pure Chemicals Industries, LTD)' that is a typical mesoporous carbon. The former and the latter were abbreviated as GAC and LAC, respectively.

2.2 Pulverization

After light crushing in a mortar by pestle, the obtained NiWC particles (referred to as P0/NiWC) were wetted with a few amount of ethanol and then pulverized in a planetary ball mill (FRITSH P7). In the pulverization, the wetted P0/NiWC was rotated together with agate balls of 15 mm ϕ in an agate vessel at 630 rpm and 3 x 10 min. The resulting fine fraction P1/NiWC was further pulverized with zirconia beads of 2 mm ϕ in the same manners as above to obtain the finer fraction P2/NiWC: Pulverization of NoWC was likewise conducted to prepare the corresponding fractions of P0/NoWC, P1/NoWC, and P2/NoWC. For GAC and LAC, crushing in a mortar was only done to obtain P0 fractions, P0/GAC and P0/LAC, respectively.

2.3 Washing with acid

P0, P1, and P2 fractions of NiWC were individually soaked in 1 M HNO₃ with stirring at room temperature for 12 h. Effectiveness of this acid treatment for the removal of nickel was already ascertained^{9,10)}. After washing repeatedly with distilled water, each acid-treated fraction, designated as P0/ANiWC, P1/ANiWC, and P2/ANiWC, respectively, was collected by filtration over a membrane filter with pore size of 0.4 μ m. The whole terminology of these acid-treated specimens was 'ANiWC'.

2.4 Morphology and properties of carbon specimens

After vacuum drying at 50°C, all of carbon specimens were examined in terms of (a) surface

Table 1 Adsorbates used for liquid phase adsorption test.

Adsorbate ^{a)}	Molecular Formula	Molecular weight	Molecular size ^{b)} (nm)	Solution		Carbon specimen (mg)
				Conc. (mg/ml)	Added amount (ml)	
MB	C ₁₆ H ₁₈ N ₃ S·Cl	319.9	0.8	0.2	20	20
AB45	C ₁₄ H ₈ N ₂ Na ₂ O ₁₀ S ₂	474.3	1.3	0.2	20	20
AB161	C ₄₀ H ₂₃ CrN ₄ Na ₂ O ₁₀ S ₂	881.7	1.7	0.2	20	20
Dx15,000	(C ₆ H ₁₀ O ₅) _n	1.5-2.0 × 10 ⁴	42.1 ± 6.0	10	5	150
Dx40,000	(C ₆ H ₁₀ O ₅) _n	3.2-4.5 × 10 ⁴	92.7 ± 15.7	10	5	150
Dx60,000	(C ₆ H ₁₀ O ₅) _n	> 6.0 × 10 ⁴	> 144	10	5	150

^{a)} See the text. ^{b)} Corresponding to the length. See the text.

state and shape, (b) particle size, and (c) pore structure, in addition to (d) the content of nickel. For (a), FESEM (JOEL JSM-5800) at 20 KV was applied to make observation at various magnifications. With (b), 50% median diameter (D50) as the average size was calculated from the distribution curve measured by laser diffractometry (FRITSH Particle Analysette 22)⁹⁾. Concerning (c), BET surface area (S_{BET}), BJH mesopore surface area (S_m), BJH micropore (the diameter is < 2 nm) volume (V_i), BJH mesopore volume (V_m), BJH macropore (the diameter is > 50 nm) volume (V_a), and total pore volume (V_t , equal to the sum of V_i , V_m , and V_a) were determined from adsorption and desorption isotherms of nitrogen at -196°C (ThermoQuest Sorptomatic 1990), as described in previous papers^{2, 8-10)}. Mean pore width (MPW), defined here as the width at 50% of V_t , was further calculated by using the accumulated curve of adsorption. The selectivity of mesopore was given as the ratio of V_m to V_t .⁶⁾ For (d), atomic absorption spectrometric analysis (HITACHI Z-8200) was made for a sample prepared by dissolving the combustible residue at 800°C with aqua regia to quantify the metal.

2.5 Liquid phase adsorption test

This test was conducted according to manners and procedures adopted by Tamai et al.¹¹⁻¹³⁾, who reported the adsorption behavior of macromolecules for mesoporous activated carbon prepared by their own ways. An aqueous solution of individual adsorbates was added to each carbon fraction in a glass-made

test tube. Employed adsorbates were three dyes of methylene blue (MB), acid blue 45 (AB45), and acid blue 161 (AB161), and three dextrans with weight-average molecular weights of 15,000, 40,000, and 60,000, denominated as Dx15,000, Dx40,000, and Dx60,000, respectively. Table 1 lists characteristics of these adsorbates together with concentrations and added amounts of their solutions, in addition to the amount of carbon, used in this test. Molecular size in the table represents the length corresponding to the longest diameter in three-dimensional directions and was calculated from linear combination of atomic orbitals for each molecule, although it is not the actual hydrated size. It may be needless to say that the three dyes are polar molecules, whereas dextrans are near-nonpolar polymers.

A glass tube containing a carbon specimen and an adsorbate solution was shaken horizontally at 200 rpm (Yamato Model SA-31) for 2 h and then centrifuged at 3,000 rpm (KOKUSAN H-103n) for 10 min. The resulting supernatant solution was collected by filtration with the above-mentioned membrane filter, and the concentration of the collected filtrate was measured by absorptionmetry (SHIMADZU MultiSpec-1500) and gel permeation chromatography (GPC, TOSOH HLC-8020 equipped with three-connecting columns of TSK gel G2500PWXL, G3000PWXL, and G4000PWXL) for dyes and dextrans, respectively. In the absorptiometric measurement, 495 nm was adopted for MB and 525 nm was for AB45 and AB161. The detector used in

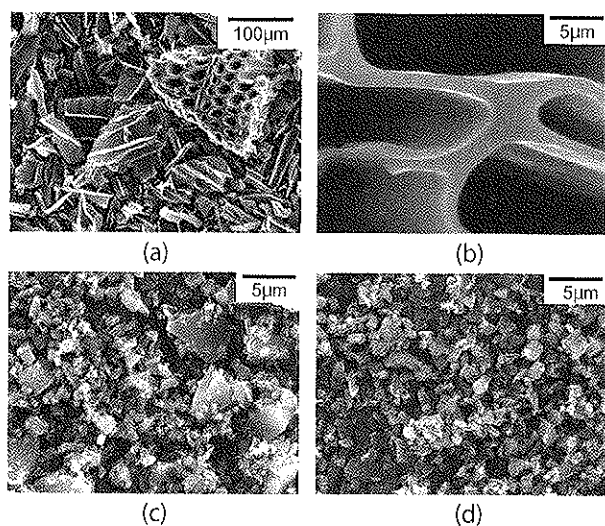


Fig. 2 SEM images of NoWC: (a) and (b) for P0, (c) for P1, and (d) for P2.

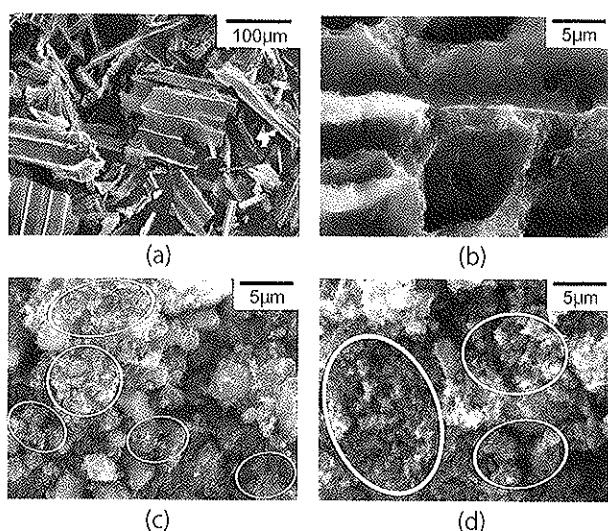


Fig. 3 SEM images of NiWC: (a) and (b) for P0, (c) for P1, and (d) for P2. Note: aggregates of raspberry-shaped particles were clearly seen in the areas, for example, encircled with white lines for (c) and (d).

GPC was a dual-flow refractometer. The adsorbed amount of each adsorbate was calculated from difference in the concentration for the initial solution and the filtrate, and the adsorption capacity was expressed in per gram carbon free from nickel. All of the adsorption tests were duplicated to obtain the average capacity as reliable data.

3. Results and Discussion

3.1 Surface state and morphology of carbon specimens

Figures 2(a)-(d) and 3(a)-(d) display typical SEM

images for NoWC and NiWC fractions, respectively. The images of ANiWC fractions are not presented here on account of their close resemblance to those of the corresponding NiWC fractions. Observation at a low magnification (Figs. 2(a) and 3(a)) made it clear that both P0/NoWC and P0/NiWC consisted of different particles in size and shape with original cell wall structure still retaining. On the other hand, highly magnified images of Figs. 2(b) and 3(b) disclosed the following serious difference for the two P0 fractions: both vertical and longitudinal cross sections were uninjured and smooth for NoWC, whereas the vertical section of NiWC was collapsed to make GNCS expose in the cell wall with longitudinal section corresponding to lumen almost undamaged. It was observed for P1 fractions given in Figs. 2(c) and 3(c) that main constituents of NoWC and NiWC were angular and 'raspberry-like' particles, respectively. For two P2 fractions comprising smaller particles with more homogeneous size and distribution compared to P1 fractions, their difference in shape became more obvious (Figs. 2(d) and 3(d)). Angularity is a typical form of pulverized carbon particles, as observed for P0/GAC and P0/LAC (Figs. 4(a) and (b)). It was needless to say that the raspberry-like shape of fragmented GNCS was quite unusual. For better understanding of the morphological change of NiWC, as well as ANiWC, related illustrations are given in Fig. 5.

3.2 Particle size, pore structure, and the content and removal of nickel

Table 2 summarizes particle size (D50) and pore structural properties for all of specimens together with the content and removal of nickel for NiWC and ANiWC. The recovery of P1 and P2 fractions relative to P0 fraction on a nickel-free basis was all over 95% irrespective of the types of wood carbons. The loss through pulverization with and without soaking in acid was thus unimportant.

For D50, $P2 < P1 < P0$ with much smaller difference for the former two fractions was common

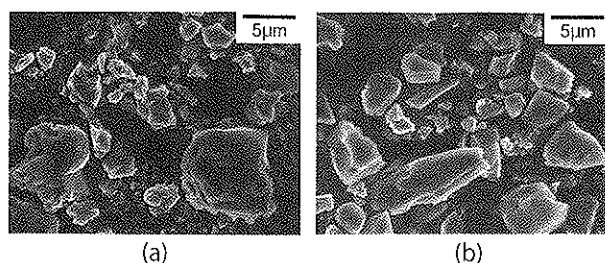


Fig. 4 SEM images of commercial activated carbons: (a) and (b) for P0/GAL and P0/LAL, respectively.

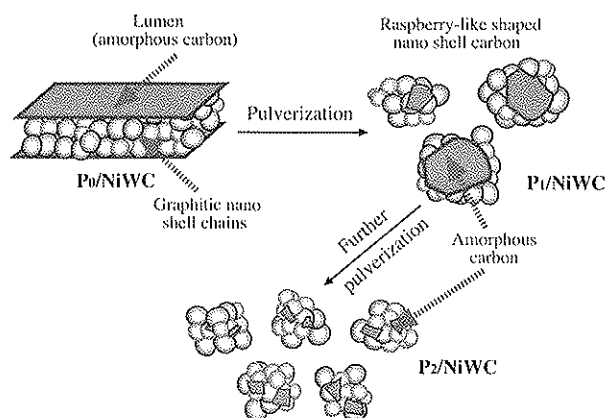


Fig. 5 Schematic presentation of the morphological change of graphitic nano shell chains (GNSC) into raspberry-shaped particles by pulverization.

to all wood carbons. This variation in the size of particles was consistent with the above-mentioned SEM observation, ensuring normal pulverization. A little larger value for ANiWC fractions than for the corresponding NiWC ones can be accounted for by coalescing minute particles during soaking in acid, as reported previously⁹⁾. Although the coalescence

concurrent with pore shrinkage described below must be unfavorable, interference in the dissolution of nickel seemed not so heavy: smaller D50 gave higher removal of the metal, although the difference was slight. Of pore properties affecting the adsorption of macromolecules, Sm is considered to be the most important because it is generally accepted as the predominant factor in determining the capacity^{11,13)}. This parameter was NoWC < NiWC < ANiWC for the same fractions, and their difference confirmed much superiority of CMC over amorphous carbon (NoWC) together with a little profit of acid treatment of NiWC. Interestingly, both NiWC and ANiWC were in the order of P1 < P2 < P0 differing from P0 < P1 < P2 of NoWC. The irregular order of CMC signifying a disadvantageous side of pulverization would have close relation to the above fragmentation of GNSC into GNS particles. For Vm that is another parameter of mesopore, NiWC and ANiWC did not differ greatly with each other and they surpassed NoWC in analogy with Sm. It was also evident that pulverization of NiWC and ANiWC gave larger increments of Vm with much larger Vm/Vt compared to that of NoWC. Although the order of Vm was P0 < P1 < P2 for any wood carbon, the concurrent increase of Va by pulverization was relatively small for CMC, thereby keeping high selectivity of mesopore. This would reflect

Table 2 Particle size, pore structural properties, and the content and removal of nickel for carbon specimens.

Specimen ^{a)}	D50 ^{b)} (µm)	SBET ^{c)} (m ² /g)	Sm ^{d)} (m ² /g)	Vi ^{e)} (cm ³ /g)	Pore structure					Nickel	
					Vm ^{f)} (cm ³ /g)	Va ^{g)} (cm ³ /g)	Vt ^{h)} (cm ³ /g)	Vm/Vt ⁱ⁾ (%)	MPW ^{j)} (nm)	Content (%)	Removal ^{k)} (%)
P0/NoWC	4.12	14	19	0.003	0.024	0.212	0.239	10.0	3	<0.1	----
P1/NoWC	0.52	73	29	0.005	0.031	0.322	0.358	8.9	4	<0.1	----
P2/NoWC	0.42	90	36	0.019	0.033	0.363	0.415	8.0	5	<0.1	----
P0/NiWC	4.15	107	174	0.001	0.204	0.391	0.596	34.2	13	7.78	0.0
P1/NiWC	0.40	137	139	0.003	0.275	0.431	0.709	38.8	25	7.73	<0.1
P2/NiWC	0.36	144	154	0.004	0.321	0.351	0.676	47.5	42	7.75	<0.1
P0/ANiWC	4.35	59	181	0.001	0.222	0.177	0.399	55.5	10	0.33	95.8
P1/ANiWC	0.89	144	154	0.003	0.232	0.294	0.529	43.8	21	0.15	98.1
P2/ANiWC	0.53	159	168	0.005	0.302	0.342	0.649	46.5	35	0.11	98.6
P0/GAC	4.50	1210	745	0.828	0.178	0.075	1.081	16.5	2	<0.1	----
P0/LAC	4.81	1310	939	0.150	1.355	0.090	1.595	85.0	4	<0.1	----

^{a)} See the text, ^{b)} 50% median diameter, ^{c)} BET surface area, ^{d)} BJH mesopore surface area, ^{e)} BJH micropore volume, ^{f)} BJH mesopore volume, ^{g)} BJH macropore volume, ^{h)} BJH total pore volume, ⁱ⁾ The selectivity of mesopore, ^{j)} Mean pore width at 50% of Vt, ^{k)} Calculated on the assumption that only the metal species was lost.

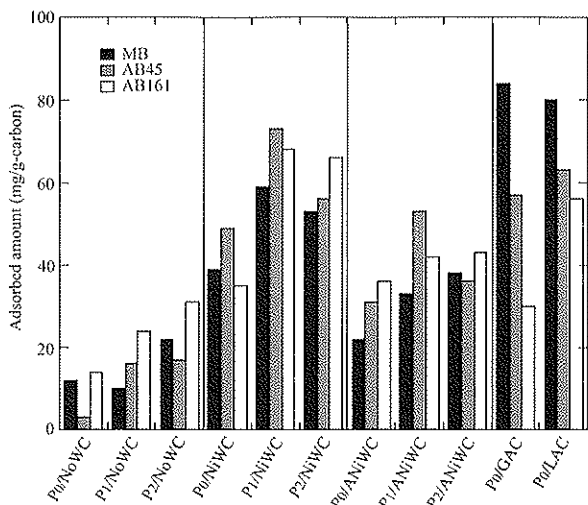


Fig. 6 Adsorption of dyes by wood carbon specimens and commercial activated carbons.

mechanical toughness of GNSC and its constituents NSC, in contrast to brittleness of amorphous carbon. In terms of the role of V_m , further attention should be paid to the close relationship with MPW. This implies that V_m can be a good index of mesopore width, so that it is likely to act as the gate for macromolecules in the liquid phase adsorption. In brief, V_m can have the function of controlling the amount of adsorbate, similarly to S_m . What is further necessary to note in relation to the likelihood was generally smaller MPW for ANiWC fractions than for NiWC ones. This can be accounted for by promoted cohesion of minute particles derived from amorphous carbon enriched with macropore in acid, according to previous finding⁸⁾. The phenomenon accompanying the decrease of macropore, affirmed by smaller V_a for ANiWC fractions, did not conflict with the concurrent increase of D50. One more important property is S_{BET} known to be critical in the adsorption of MB^{14,15)}. This parameter is expected to have appreciable influence on the adsorption of other dyes with low molecular weight than MB, for all that substantial participation of S_m in the treatment of AB45 and AB161 was already reported¹¹⁻¹³⁾. Excepting the extraordinary low value for P0/ANiWC reflecting the aforesaid serious shrinkage, S_{BET} was analogous to S_m and V_m in that CMC was much larger than

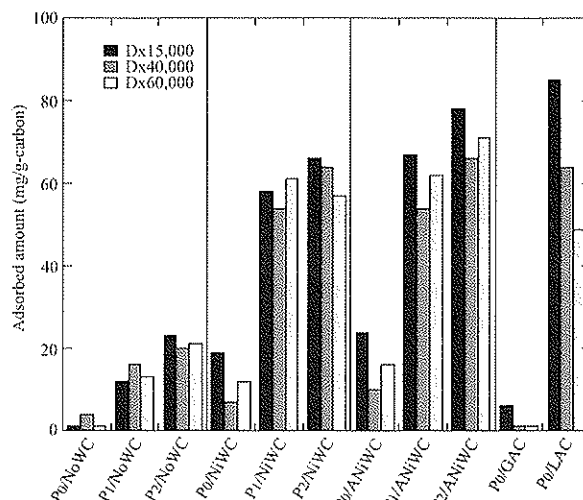


Fig. 7 Adsorption of dextrans by wood carbon specimens and commercial activated carbons.

amorphous carbon. Concerning P0/GAC and P0/LAC, the former was well characterized by quite large S_{BET} and V_i , and the latter was by extremely large S_m and V_m together with high V_m/V_t . Although these characteristics made sure high aptitude of their own use, it was evident that even P0/LAC compared unfavorably with NiWC and ANiWC in MPW.

3.3 Adsorption of dyes and dextrans

Figures 6 and 7 depict adsorption capacities of all carbon specimens for dyes and dextrans, respectively. In the adsorption of dyes by P0/GAC and P0/LAC, the amounts were in the order of AB161 < AB45 < MB. Although this order showed strong dependence on the molecular size of adsorbates (Table 1), the quantity of MB was larger for GAL than for LAC and those of AB45 and AB161 were opposite. Collation with structural data given in Table 2 made it possible to interpret that S_{BET} and S_m would play the predominant roles in the adsorption of MB and two ABs, respectively. A similar interpretation held for NoWC with P0 < P1 < P2 in the adsorbed amount of any dye. As for NiWC and ANiWC, their larger adsorption capacities than that of NoWC were not easily elucidated because the order of P0 < P2 < P1 in the general amount was not always correlated with S_{BET} and/or S_m , and was not compatible with V_m and MPW, either.

The irregularity in the order can be understood by assuming some disadvantage concurrent with pore structural and morphological changes. That is, it seemed valid to explain that the effect of increase in V_m and MPW, and/or the transformation of GNSC into NSC particles exceeded the disadvantage for P1, while the situation was reversed for P2 with prolonged pulverization. The presence of nickel was favorable, since NiWC was larger than ANiWC in the general adsorption capacity. In connection with this aspect, smaller MPW for ANiWC than for NiWC would be less handicapped, judging from the adsorption of dextrans discussed below. It is also important that three dyes are polar adsorbates. When considering these matters, the most plausible candidate for the relevant factor was increase of oxygen-containing groups¹⁶⁻¹⁸⁾ occurred on the carbon surface, as exemplified by the assumed depiction (Fig. 8). The adsorbed amounts of dextrans were, on the other hand, far larger for PO/LAC than for PO/GAC. This can be attributed to difference in not S_m but V_m , or the width of mesopore between them. Actually $Dx60,000 < Dx40,000 < Dx15,000$ in the amount for PO/LAC was the order expected from their molecular sizes (Table 1). For three wood carbons, $PO < P1 < P2$ in the general capacity agreed with the order of MPW. More noticeable was the superiority of ANiWC over NiWC. The opposition to the above situation of dyes would realize under the following circumstances: i) elimination of coexistent nickel facilitated the access of dextrans, ii) oxygen-containing groups did not have serious influence on the adsorption of such near-nonpolar giant molecules, iii) so that, mesopore width could be the predominant factor, iv) smaller MPW for P1/ANiWC and P2/ANiWC than that for the corresponding NiWC fractions was, however, no longer inconvenient probably because the mesopore width for the former attained to an sufficiently large level. It should be emphasized that P2/ANiWC had the highest capacity among wood carbon fractions to surpass PO/LAC

in the amounts of $Dx60,000$ and $Dx40,000$ with a little inferiority of $Dx15,000$. The satisfactory capacity of this specimen was principally afforded through pulverization, as was ascertained by rather small difference in the capacity for NiWC and ANiWC fractions and considerably large difference between P0 and P1 fractions of both NiWC and ANiWC. The fact in turn confirmed that this post-treatment to produce a number of raspberry-shaped NSC particles, thereby making the accessibility of giant macromolecules greatly enhance was so effective as to compensate for the big drawback of much smaller S_{BET} , S_m , and V_m than those of PO/LAC. According to the above adsorption of dyes, P1 and P2 of NiWC were equal or superior to PO/LAC in the amount of AB45 and AB161. The sufficiently high capacity, however, came from the presence of nickel that is an environmentally unfriendly and expensive metal, and hence, the practical utilization of NiWC is limited. On the contrary, the application of ANiWC causing no serious trouble as the adsorbent for non-polarized polymers is promising. In addition, increase in the adsorption capacity after removal of nickel by soaking in acid for its recovery and reuse is industrially preferable. Nevertheless, complete elimination of the metal was not achieved at the present stage. It is also necessary to tell that irrespective of acid treatment, the present pulverization of NiWC yielded minute particles with diameter of < 0.1 mm, which is hard to handle, in a considerable percentage. Efficient reduction in the

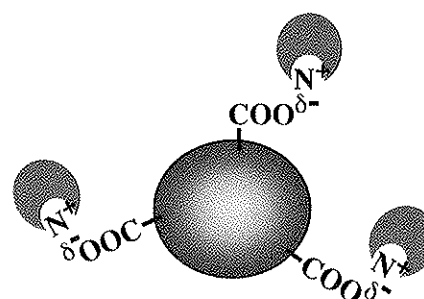


Fig. 8 Assumed adsorption of dye molecules on pulverized carbon particles.

particle size of CMC without losing the morphological feature of GNSC is thus required from a practical viewpoint. Although detailed mechanism of the adsorption by NiWC and ANiWC is also needful to be investigated, development of such improved post-treatments is the preferential subject in our further study.

4. Conclusions

The present study examined influence of pulverization followed by washing with acid as post-treatments for CMC obtained by 900°C-carbonization of nickel-loaded larch on liquid phase adsorption of dyes and dextrans. When pulverized, GNSC as the crystallized morphology of CMC was collapsed into fragmented NSC particles with raspberry-like shape, accompanied by increase of V_m and MPW, or enlargement of mesopore width. Subsequent washing with acid to remove nickel caused considerable shrinkage of large pore with a little decrease of mesopore width. Although pulverized CMC was superior to LAC in the adsorbed amounts of such dyes as AB45 and AB161, the good capacity depended greatly on the presence of the metal. On the other hand, pulverized and acid-treated CMC was generally superior to the activated carbon in the capacity of dextrans. Because the removal of nickel is industrially preferable, pulverization and subsequent washing with acid are promising post-treatments of CMC for producing a practical adsorbent for non-polar polymers.

Acknowledgments

This work was supported by a Grant-in Aid for Scientific Research (14560128) from the Ministry of Education, Culture, Sports, Science and Technology, Japan.

References

1) Suzuki K., Yamada T., Suzuki T. (2007) *Zairyo*, **56**, 339-344

2) Suzuki T., Suzuki K., Takahashi Y., Okimoto M., Yamada T., Okazaki N., Shimizu Y., Fujiwara M. (2007) *J. Wood Sci.*, **53**, 54-60

3) Suzuki K., Matsuzaki H., Yamada T., Suzuki T. (2008) *Trans. MRS-J*, **33**(4), 833-836

4) Suzuki T. (2008) *Chemical Engineering*, **53**(2), 57-60

5) Suzuki K., Suzuki T., Takahashi Y., Okimoto M., Yamada T., Okazaki N., Shimizu Y., Fujiwara M. (2009) *J. Wood Sci.*, **55**, 60-68

6) Suzuki K., Suzuki T., Takahashi Y., Okimoto M., Yamada T., Okazaki N., Shimizu Y., Fujiwara M. (2005) *Chem. Lett.*, **34**, 870-871

7) Suzuki K., Suzuki T., Saito Y., Kita H., Sato K., Konno T. (2009) *TANSO*, No. **239**, 169-171

8) Suzuki K., Yamada T., Saito Y., Suzuki T. (2008) *Mokuzai Gakkaishi*, **54**, 333-339

9) Suzuki K., Suzuki T., Takazawa N., Funaoka M. (2008) *Holzforschung*, **62**, 157-163

10) Suzuki T., Matsuzaki H., Suzuki K., Saito Y., Yasui S., Okazaki N., Yamada T. (2008) *Chem. Lett.*, **37**, 798-799

11) Tamai H., Kakii T., Hirota Y., Kamamoto T., Yasuda H. (1996) *Chem. Mater.*, **8**, 454-462

12) Tamai H., Ikuchi M., Kojima S., Yasuda H. (1997) *Ad. Mater.*, **9**, 55-58

13) Sasaki M., Tamai H., Yoshida T., Yasuda H. (1998) *TANSO*, No. **181**, 20-26

14) Tseng R.L., Wu F.C., Juang R.S. (2003) *Carbon*, **41**, 487-495

15) Hasegawa T., Abe I. (2005) In: H. Yoshida (ed), *Handbook on Porous Adsorbents*, Fuji Tecnosystem, Tokyo, p.71

16) Lin S.H. (1993) *J. Chem. Tech. Biotechnol.*, **58**, 159-163

17) Newcombe G. (1994) *J. Colloid Interface Sci.*, **164**, 413-420

18) Tamai H. (2005) In: H. Yoshida (ed), *Handbook on Porous Adsorbents*, Fuji Tecnosystem, Tokyo, p.147

(Received 27 Sep. 2010, Accepted 10 May. 2012)

**【研究報告】 カラマツの 900℃ニッケル触媒炭化で得られた結晶性メソ孔
木質炭素の染料とデキストランの液相吸着**

**鈴木 勉 * ** ** ** **, 鈴木京子 *, 服部和幸 *, 岡崎文保 *, 斎藤幸恵 **,
喜多英敏 ***, 玉井久司 ******

概要：カラマツの 900℃ニッケル触媒炭化で得られた結晶性メソ孔木炭（CMC）について、染料とデキストランの液相吸着能を粉砕 - 酸洗浄の前後で調べた。粉砕すると CMC の結晶形態であるグラファイトナノシェルチェーンはラズベリー型のナノシェル炭素に分解すると共にメソ孔の体積と径が増大した。これらの形態と細孔構造変化は両吸着物の吸着量を大きく増加させた。引き続き共存ニッケル除去のための酸洗浄はデキストランの吸着量をさらに増加させ、市販のメソ孔炭素の性能を上回った。回収、再使用のためのニッケル除去は工業的にも好ましいので、粉砕と引き続き酸洗浄は CMC からの非極性高分子吸着剤の実用生産に適した後処理であった。

キーワード：結晶性メソ孔木炭, グラファイトナノシェルチェーン, 液相吸着能, 粉砕, 酸洗浄